Hurst-Exponent-Based Detection of High-Impedance DC Arc Events for 48-V Systems in Vehicles

Yousef Abdullah, *Student Member, IEEE*, Jamie Shaffer, Boxue Hu, *Member, IEEE*, Bailey Hall, Jin Wang, *Senior Member, IEEE*, Amin Emrani, *Member, IEEE*, and Babak Arfaei

***Abstract*—Expanding dc electrical distribution systems require improved detection and mitigation of dc arc events. The high heat resulting from dc arcing raises concerns on equipment and personnel safety. In this article, a new adaptive detection method for series dc arc faults is presented. The proposed detection method utilizes Hurst exponent estimation of the system current to detect arcing events with a high detection rate and strong immunity against sudden load changes, chaotic load profiles, and switching harmonics. To verify the proposed detection method, a test setup to generate dc arcs was built, and over one thousand tests were performed under various conditions. The tests were conducted under different environment temperatures, air gap lengths, loads, and electrode diameters. The effectiveness of the proposed method is demonstrated by the test results and validated with an arc detector prototype.**

***Index Terms*—DC arc, fast Fourier transform (FFT), Hurst exponent, wavelet.**

I. Introduction

DC ELECTRICAL distribution systems are being widely adopted for various applications, including photovoltaic-based microgrids, electric vehicles, and aircraft. DC systems are prone to dc arcing events, which need to be detected and terminated before extensive damage is caused to equipment. Unlike ac currents, dc currents have no zero crossing, making sustained arcs more likely to occur. Sustained dc arcs have safety concerns as they generate high temperatures and inject electromagnetic interference into the system. To avoid damage to equipment and improve the safety of these systems, reliable detection and protection methods against dc arcing events are needed.

DC arcs can be categorized into high-impedance (series) and low-impedance (parallel) arcs. Low-impedance arcs are often caused by the air breakdown between conductors at different potentials and lead to large short-circuit currents, allowing them to be easily detected. High-impedance dc arcs are generated when there is a loose connection or an electrical conductor carrying an electrical current splits into two. As the cable splits, an arc occurs and reduces the current flowing through the circuit due to its high impedance. High-impedance arc detection is more challenging due to its similarity in lowering the current to a load change (e.g., reduced load). This challenge can be observed in noisy environments, such as in a vehicle, where loads are constantly switching. Distinguishing an arc from a load change, a load with switching noise, or loads with chaotic behaviors is important for safe and reliable operation of the vehicle.

Mild hybrid electric vehicles (MHEVs) with 48-V belt starter generators have been developed to achieve higher fuel efficiency than the existing 12-V-based systems [1]–[3]. They use a dual-voltage configuration (12 V, 48 V) interconnected with a bidirectional dc–dc converter to deliver the needed energy to the different loads in the vehicle. Due to the higher system voltage of MHEVs, investigation of dc arcs and protection is needed.

Many empirical methods for dc arc detection have been proposed. Zonal-based detection [4]–[7] divides the system into several branches and monitors the current of every load. Unplanned changes in the current are then used to identify arcing events. These methods rely primarily on hardware sensors distributed throughout the system to collect and process the data for arc detection. Various statistical methods have also been developed to detect the arc signature by analyzing databases of arc data [8]–[14]. However, most of the proposed statistical methods are prone to mis-triggering by chaotic load profiles due to their noisy behavior and similarity to dc arcs. Wavelet and fast Fourier transform (FFT) methods [12], [15]–[19] are also known to be implemented for dc arc detection in a variety of applications. These software-based methods scan the frequency spectrum for new noisy behavior. To avoid switching noise mis-trigger, a specific frequency band is selected, where switching noise is absent or predefined. However, this would limit their application and ability to avoid mis-trigger due to switching noise in case of a load change. Machine learning [20] and pattern matching [21] algorithms were also introduced to detect arcs. Machine learning is known to be complex and requires heavy calculations, which significantly increases the cost of the system. This article proposes a new detection method [22], [23] for dc arcs with lower calculation load and high immunity to switching noise and chaotic loads. The method is validated by

Manuscript received December 3, 2019; revised March 24, 2020 and May 30, 2020; accepted June 21, 2020. Date of publication September 1, 2020; date of current version November 20, 2020. Recommended for publication by Associate Editor A. J. Marques Cardoso. *(Corresponding author: Yousef Abdullah.)*

Yousef Abdullah, Jamie Shaffer, Boxue Hu, Bailey Hall, and Jin Wang are with the Department of Electrical and Computer Engineering, The Ohio State University, Columbus, OH 43210 USA (e-mail: abdullah.67@buckeyemail.osu.edu; shaffer.607@osu.edu; hu.990@osu.edu; hall.2499@osu.edu; wang.1248@osu.edu).

Amin Emrani and Babak Arfaei are with the Research and Advanced Engineering, Ford Motor Company, Palo Alto, CA 94304 USA (e-mail: amin.emrani@gmail.com; barfaei@ford.com).

Color versions of one or more of the figures in this article are available online at https://ieeexplore.ieee.org.

Digital Object Identifier 10.1109/TPEL.2020.3020587

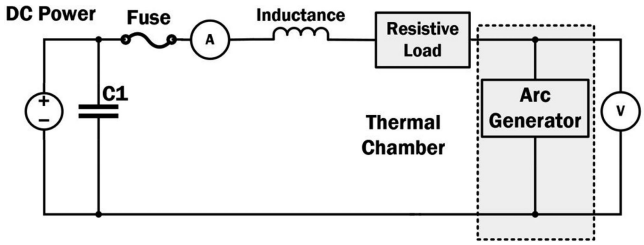

Fig. 1. Copper electrodes and dc arcing event.

TABLE I
TEST CONDITIONS

Voltage	48 V
Load Power	400 – 2000 W
Electrodes Diameter	1.5 – 4.8 mm
Gap Length	1 – 4 mm
Sampling Frequency	1 MHz
Environment Temperature	$-20^{o}C, 25^{o}C, 150^{o}C$

using hundreds of dc arc samples generated through hardware tests. This article starts with building an arc generator to perform tests and create a database of arcing events. In the second section, the Hurst exponent is introduced. The detection algorithm is then proposed and validated using the arcs database. Finally, the method is implemented in a digital signal processor (DSP) for live detection of dc arcs.

II. Test Setup and Types of DC Arcs

A test setup is established to generate dc arcs at various conditions. This is achieved by using two copper electrodes fixed on a moving slider. Initially, the copper electrodes are connected forming a closed-loop circuit. High current is conducted through the electrodes and controlled using switchable resistive loads. When the electrodes separate, the inductance of the system causes a high-voltage overshoot across the electrodes, which results in the breakdown of the air between the electrodes, generating a high-impedance arc. Hardware test results have shown that circuit parameters such as cable impedance, load impedance, and source power have effects on the arcing profile [14], [24]. Nonelectrical parameters such as electrode type, separation speed, and temperature can also affect the arc characteristics.

A. Hardware Tests and Data Collection

The dc arc test setup diagram is shown in Fig. 1. The arc generator is a mechanical slider holding two electrodes actuated with a stepper motor and a control board. The separation speed as well as the air gap length are both controlled by the stepper motor. A thermal chamber is used to encapsulate the arc generator to accurately control the environment temperature at −20, 25, and 150 °C. Figs. 2 and 3 show the arc generator with the thermal chamber as well as an arcing event. The test conditions for the dc arc tests are shown in Table I. The system voltage is chosen to be 48 V, which is widely used in MHEVs. An inductor of

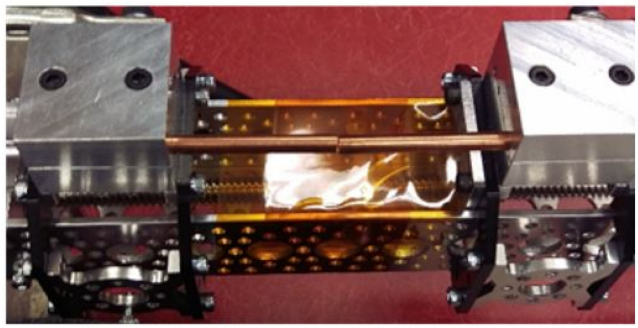

(a)

(b)

Fig. 2. Arcing event. (a) Before arcing. (b) During arcing.

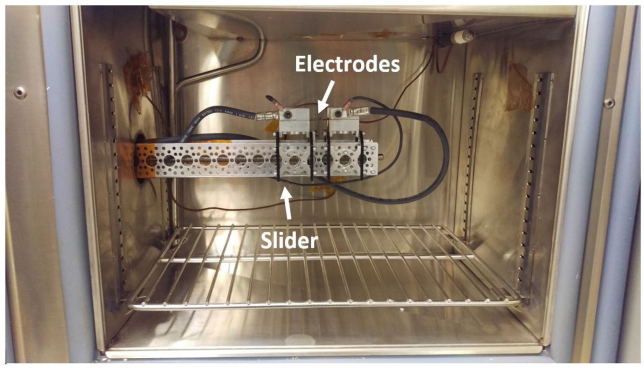

Fig. 3. Arc generator inside a thermal chamber for ambient temperature control.

10.3 μH is connected in series with the resistive load. This inductance simulates the vehicle cable inductance. The tests were performed at different air gap lengths from 1 to 4 mm at a constant separation time of 2 s. A total number of 930 dc arcs tests were performed, and both the voltage and current data were collected at a sampling frequency of 1 MHz. The data are used later to test and tune the proposed detection method.

B. Types of Arcing Events

Through the arcing tests, three types of arcing events were identified: sustainable arc, intermittent arc, and unsustainable arcing. These arcing events are illustrated in Figs. 4 and 5.

1) *Sustainable arc:* It represents an arcing event, which reaches steady state and lasts during the entire arcing test time, which is 5 s.

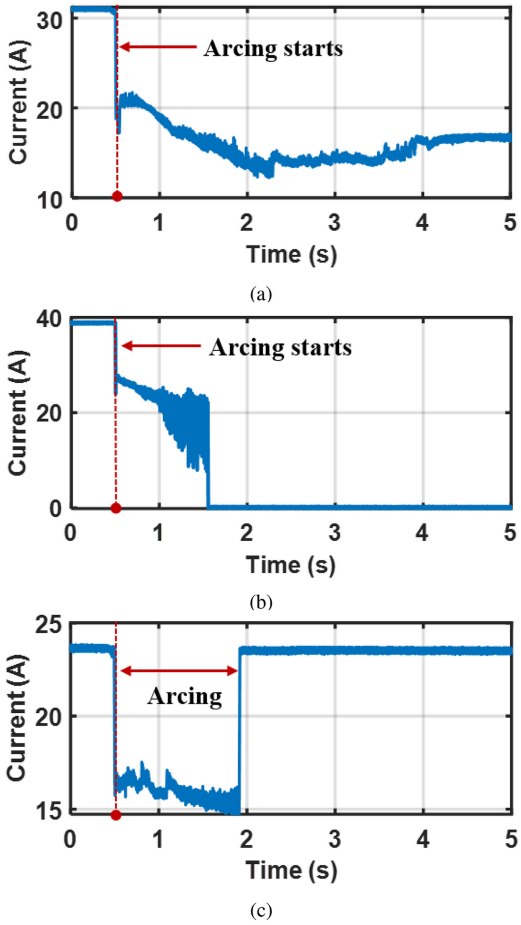

Fig. 4. Types of arc events. (a) Sustained arc. (b) Unsustained arc. (c) Intermittent arc.

2) *Intermittent arc:* It is an arc that occurs for a very short period. During this time, the electrodes melt and reconnect forming a closed circuit and extinguishing the arc. These arcs normally occur when the current is high compared to the thickness of the electrodes and the gap distance is less than 2 mm.
3) *Unsustained arc:* It is an arcing event that does not reach steady state and stops after a few seconds. Unsustainability could be due to low current and large gap distance.

III. Introduction to the Hurst Exponent

DC arc events inject a wide range of frequencies into the electrical current spectrum. The sudden chaotic behavior of the resulting arc waveforms can be detected if a method can measure the level of randomness or the chaos of the signal. Such a noisy behavior has similar characteristics to a human brain's neural activity. In [25], the Hurst exponent method was proposed to detect epileptic seizure in a brain by examining the brain's electroencephalogram signals. The similar chaotic behavior of the seizure neural signals to arc events led to the investigation and development of the proposed arc detection method, which utilizes the Hurst exponent estimation.

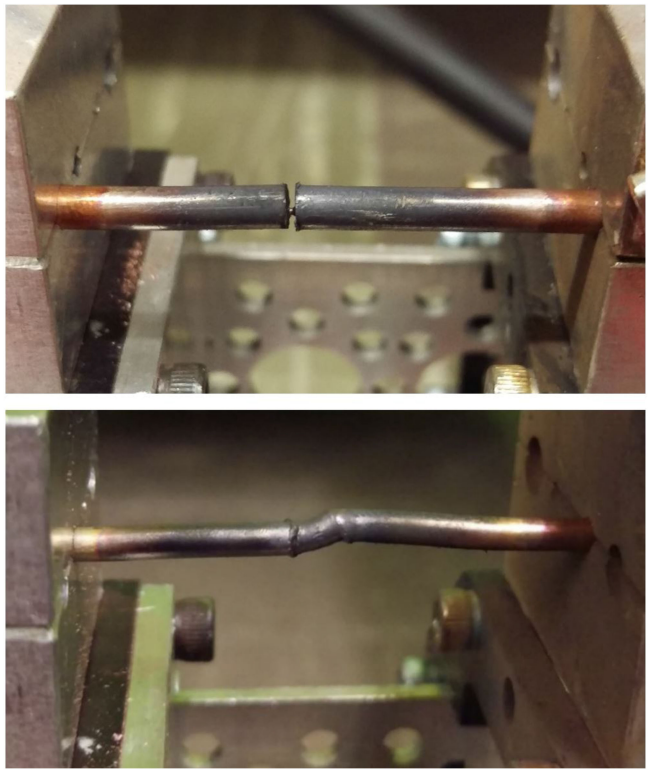

Fig. 5. Reconnected electrodes due to electrode meltdown.

The Hurst exponent is a mathematical tool used to predict the trend of fluctuating data [26]. Based on long-term memory analysis, the Hurst exponent can be used to determine the randomness level of a data series. It can identify random, positively correlated, and negatively correlated signals by calculating the rate of change of the standard deviation in a time series.

The Hurst exponent is derived from Brownian motion, which is defined as a random movement with normal distribution and zero mean. A cumulative position $X(t)$ with zero expected value can be written as

$$E(X(t) - X(0)) = 0 \tag{1}$$

$$[E(X(t) - X(0))^2]^{0.5} \propto t^{0.5} \tag{2}$$

$$[E(X(t) - X(0))^2]^{0.5} \propto t^{H} \tag{3}$$

where $E(X(t))$ is the expected value of $X(t)$ and H is the Hurst exponent.

From (2), the standard deviation of the random position grows with time with an exponent of 0.5. By generalizing the equation, as in (3), this concept can be used with any data series other than a Brownian motion using different values of H representing a nonrandom data.

The values of H can range from 0 to 1. As per (2), an H value of 0.5 represents random data. An H value of 1 or 0 represents positively and negatively correlated data, respectively. The Hurst exponent value for a given data is usually estimated by using a numerical method. Several methods have been developed to estimate the value of H. The dispersional analysis method [27]

is used in this article for the Hurst value estimation due to its lower calculation requirements. From (3), the Hurst value can be estimated by

$$[E(X(t) - X(0))^2]^{0.5} = Ct^H \tag{4}$$

$$\log[E(X(t) - X(0))^2]^{0.5} = H\log(t) + \log(C) \tag{5}$$

where (C) is a constant. (H) is found by curve fitting (5) to the data. The slope of the curve is the Hurst exponent value.

In this article, the Hurst exponent values are used to detect abnormal behaviors in the data of current measurements. Depending on the behavior type, the proposed algorithm decides whether the abnormality is due to an arc or not. This is explained in the next section.

IV. Proposed Detection Method

In this section, the Hurst-exponent-based detection method is explained. The concept of the detection method consists of three main steps: 1) data collection; 2) data filtering; and 3) data analysis. First, the data are collected using a current sensor and then passed through the filtering stage. After the data are properly filtered, the Hurst exponent analysis is applied. The Hurst exponent determines the level of randomness or chaos of the data. If the randomness level of the data suddenly changes when compared to the system long-running Hurst average, an arc is detected. This section is organized as follows: 1) data filtering and conditioning and 2) Hurst analysis and the overall algorithm.

A. Data Filtering and Conditioning

A proper filtering process is a crucial step for proper arc detection. There are two proposed filtering stages before the data are analyzed for arc signature: a bandpass filter (BPF) and an envelope detector. The BPF is used to filter out low-frequency components resulting from some load profiles, as well as loads with high transients such as a sudden load change.

Switching loads on the vehicle are a source of undesired noise, which affects the performance of detection methods. The noise injection of switching loads may cause false positives or missed arcs for frequency based methods such as the wavelet or the FFT. Unless these switching frequencies are predefined, a proper filtering technique is needed to reduce the noise energy in case it falls within the BPF range. To achieve switching noise energy reduction, the envelope filter is proposed, which is the second-stage filtering.

The envelope filter is applied by taking the outline of the bandpass (BP)-filtered signal, significantly reducing the switching energy. The reduction of switching harmonics allows the detection method to be more sensitive to arc fluctuations over the selected time window. To illustrate this, Fig. 6 shows an BP-filtered arcing event occurring at $t = 0.5$ s. The current contains switching noise falling within the BPF range. Because the switching energy is much higher than the arcing energy, the arc is harder to detect. To reduce the switching energy, the upper signal envelope is applied, as shown in Fig. 7, to the BPF output. As a result, most of the switching energy is removed making the arc energy dominant and detectable by the Hurst method. The proposed method has the advantage of not having to define loads behavior or switching frequencies prior to the vehicle operation.

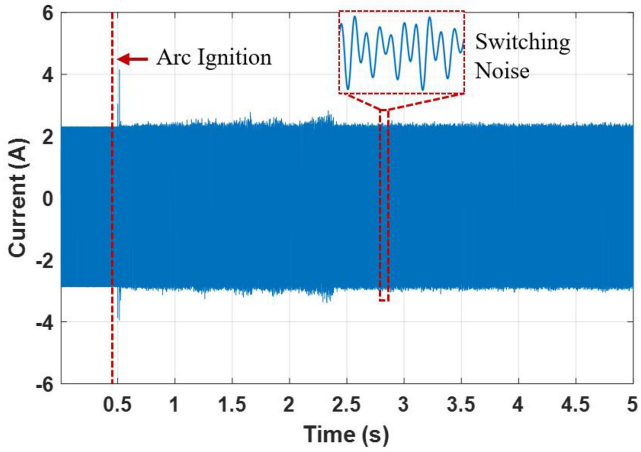

Fig. 6. BP-filtered arc with switching noise. The switching noise energy is higher than the arc energy.

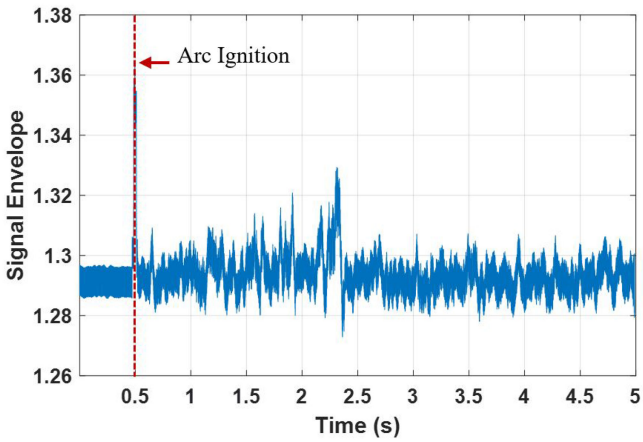

Fig. 7. Envelope filter output. The arc energy is higher than the switching noise energy.

The envelope filter is implemented by taking a moving window of data points and calculating the rms value for each window. The window size should be smaller than the Hurst window and larger than the period of the BPF lower cutoff frequency. Based on experimental tests, a window size of 1/4 of the Hurst window was used, which is 6.25 ms.

After the BPF and the envelope are applied, the resulting data output is a signal with a constant value (assuming no arc or other noise exist). However, because Hurst exponent measures the randomness of a signal, calculating the Hurst exponent yields a Hurst value of 1. Small amount of white noise must be added to the signal to make the Hurst values converge to 0.5. The next stage after the filtering is the Hurst exponent calculation of the signal data, which is discussed in the next subsection.

B. Hurst Analysis

The Hurst analysis, when applied to a dc current signal with white noise, yields values of about 0.5 because of the

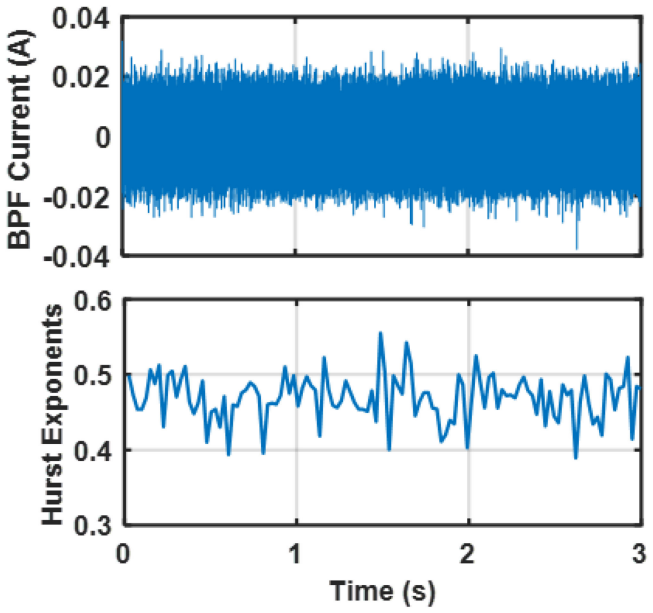

Fig. 8. Hurst exponents of a filtered constant dc current with white noise stabilizing around 0.5.

randomness of the signal background noise. This is illustrated in Fig. 8, where a constant dc current (filtered with a BPF) is shown with the corresponding Hurst values. Because the arcing event changes the profile of the current waveform and injects a wide range of frequencies, the Hurst exponent can be used to detect any change or fluctuation resulting from the arc ignition.

The time window size of the analyzed data correlates with how the Hurst values respond to the data. Each Hurst exponent value is calculated for a specific time window. Changing the time window directly affects the values of the exponents. For example, a high-frequency oscillation in a large time window is seen as a random event causing the exponents to converge to 0.5, while the same oscillation at a very relatively small time window is seen as a rising or falling signal (which is not random), causing the exponents to diverge from 0.5. Because fast arc detection is always desired, the time window chosen for the single Hurst exponent calculation is 25 ms. The detection of an arcing event is based on changes in multiple Hurst exponent windows compared to the running long averaged exponent value of the system.

The detection algorithm starts by collecting and filtering a time window of data using the BPF and the envelope. During the filtering stage, the dc component, low-frequency transients, and high-frequency transients are removed or attenuated from the data. After the filtering stage is completed, the Hurst exponent estimation is performed. The Hurst value is then compared to the long running average of previous exponents. If a sudden change exceeding the predefined threshold value is detected, an arc event has occurred. The number of windows used for detection can be determined based on the designer requirements. More windows result in longer detection time with less susceptibility to noise. The method diagram is shown in Fig. 9, where H_n is the nth Hurst value, H_{avg} is the long running average Hurst value of the system, and ΔH_{th} is the threshold change in Hurst values for arc detection.

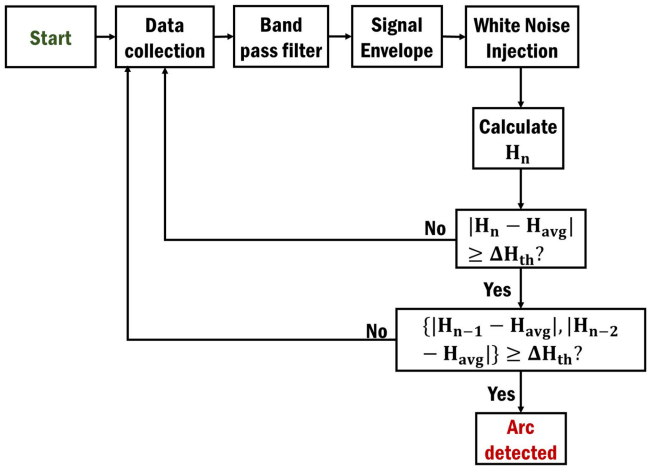

Fig. 9. Proposed detection method block diagram.

TABLE II
PROPOSED METHOD PARAMETERS

Band Pass Filter	10 kHz – 20 kHz
Envelope Window	6.25 ms
Hurst Window	25 ms
Exponent Threshold ΔH	0.2
Number of windows for detection	3 windows
Detection time	75 ms

The hardware tests performed in Section II were used to test, validate, and tune the algorithm. The parameters of the detection algorithm are shown in Table II. Two samples are shown in Figs. 10 and 11 with the input to the algorithm (current data) and the output of the algorithm (Hurst exponents). The arcs are shown with the corresponding Hurst values after filtering. As the arc starts at $t = 0.5$ s, a sustained step change above the threshold in the Hurst exponent values for two or more windows indicates the arc event.

V. PERFORMANCE VALIDATION OF THE PROPOSED METHOD

In many applications, several system conditions and events can affect arc detection methods. Sudden load changes, for example, with high di/dt inject a wide range of frequencies into the system. Immunity against these abnormal events is essential for reliable and robust detection. In this section, the proposed detection method is tested under various abnormal conditions, including sudden load changes, chaotic load profiles, and switching noise. In addition, the calculation load and detection rate of the method are also presented.

A. Load Transient Analysis

Detection of arcing events is based on the Hurst exponent change and number of windows used. Load changes cause high frequencies to be injected into the system. Immunity against load changes is desired to avoid false triggering. The proposed

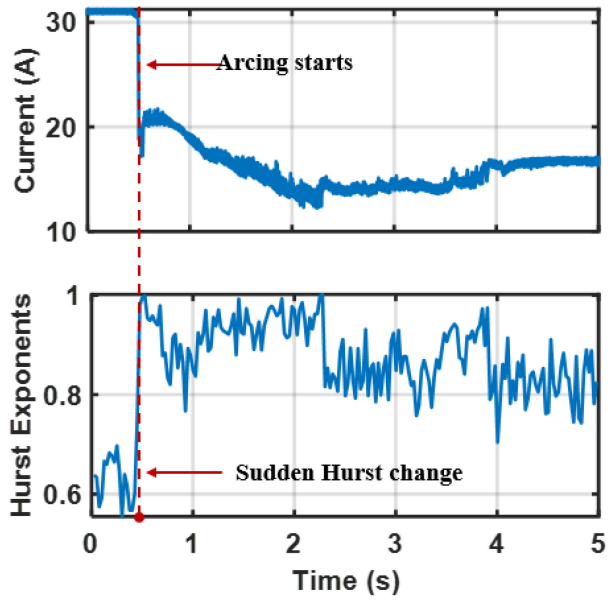

Fig. 10. Sample (1) dc arc occurring at $t = 0.5$ s with corresponding Hurst exponents.

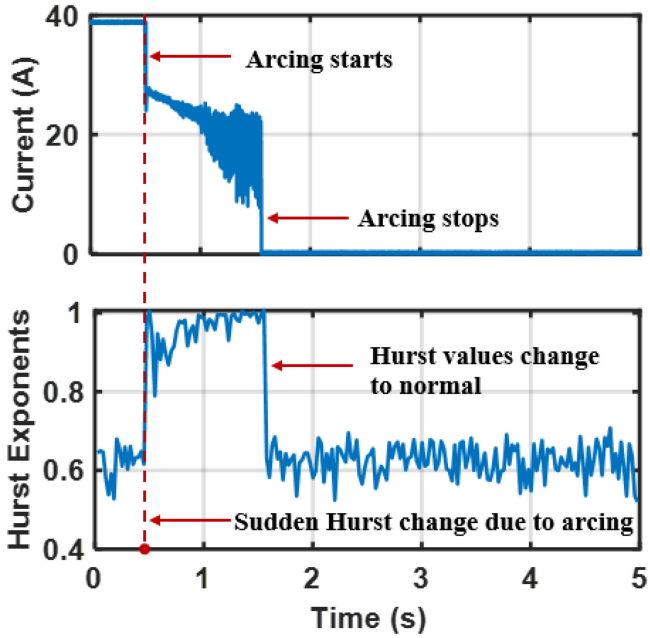

Fig. 11. Sample (2) dc arc occurring at $t = 0.5$ s with corresponding Hurst exponents.

method was tested using two types of loads: sudden load changes and chaotic load profiles.

Load transients could occur with a slow or high di/dt. Loads with slow rise time have no effect on the method as they are filtered out by the BPF. In contrast, loads with high di/dt could result in a sudden spike in the Hurst exponent values, as shown in Fig. 12. However, these loads are avoided by using more than a single time window. The number of windows with high Hurst values decides whether an arc is detected. To avoid false

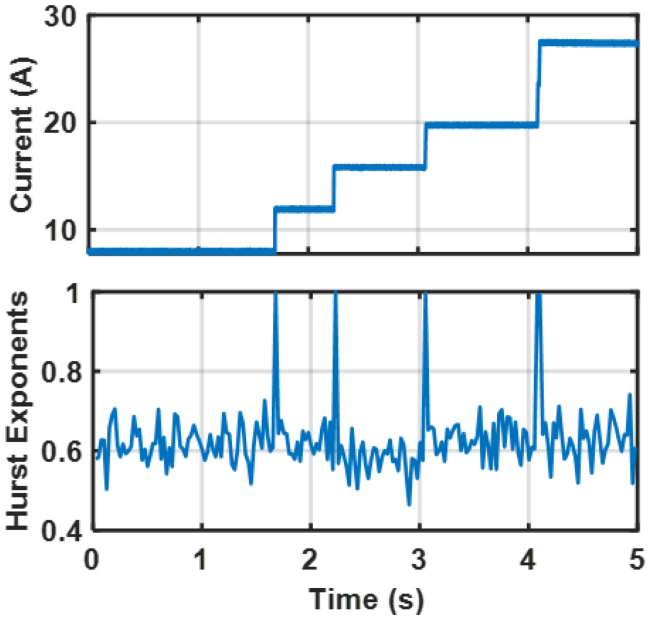

Fig. 12. Sudden load change effect on the Hurst exponents. No false trigger occurs as the Hurst spikes do not satisfy the detection time threshold of two windows (50 ms).

triggering, the combined time of the Hurst windows need to be longer than the load change transient time. This ensures that load changes will not cause high Hurst values during all the selected Hurst windows. A minimum of two windows (total time: 50 ms) are needed to avoid load transients false triggering.

Another type of loads is a chaotic load profile. In a vehicle, driving and steering result in a chaotic current being generated and consumed by various loads. By obtaining several electric vehicle load profiles, the immunity against chaotic loads is tested. Due to the low frequency nature of these profiles (less than 10 kHz), the BP filtering stage proved sufficient to stop any miss-trigger events, as shown in Fig. 13. High transients in the current resulted in single spikes on the Hurst values plot, which does not false triggers the method. Only a sustained step change that is larger or equal to two consecutive Hurst values (adjustable) satisfies the detection threshold value. Fig. 14 shows a zoomed-in plot of Fig. 13 in the time period 1–8 s for better visual analysis.

B. Switching Harmonics Immunity

Switching loads are widely used in vehicles and other electrical distribution systems. Unlike other methods, the proposed detection method has high immunity to switching harmonics. Through the proposed envelope filtering, switching harmonics energy is significantly reduced (see Fig. 6 and 7), ensuring that only arc-ignition energy is large enough to satisfy any detection threshold. If the switching energy is still significant, no false triggering can occur because the detection method recognizes it as background noise. To illustrate this, Fig. 15 shows a dc arcing event occurring at $t = 0.5$ s. Switching harmonics were injected in the waveform using MATLAB, with a magnitude of 15% of the dc current inside the BPF range at a frequency of 15 kHz

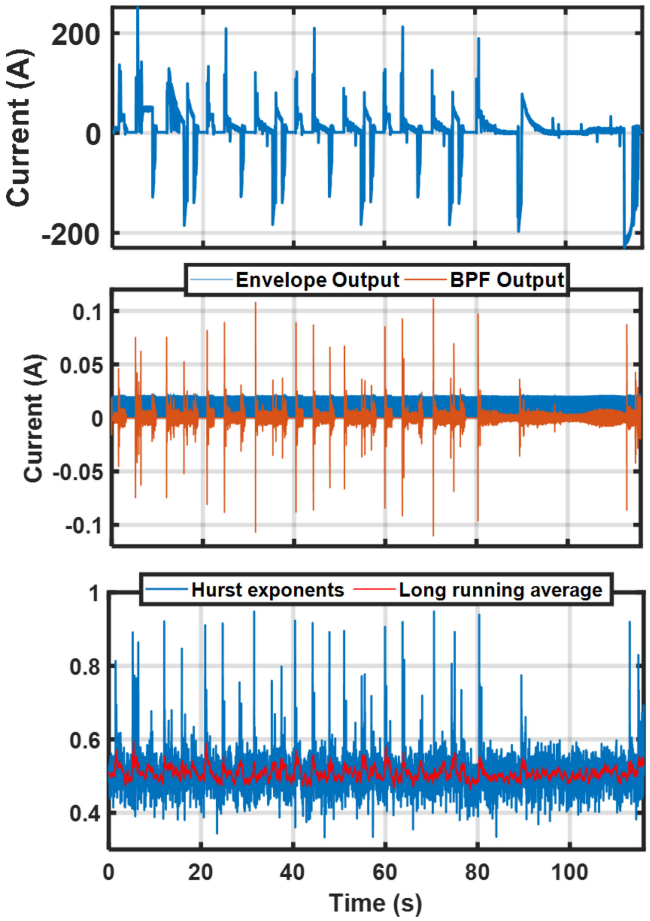

Fig. 13. Chaotic load profile immunity. No false trigger occurs as the Hurst spikes do not occur in two or more consecutive windows.

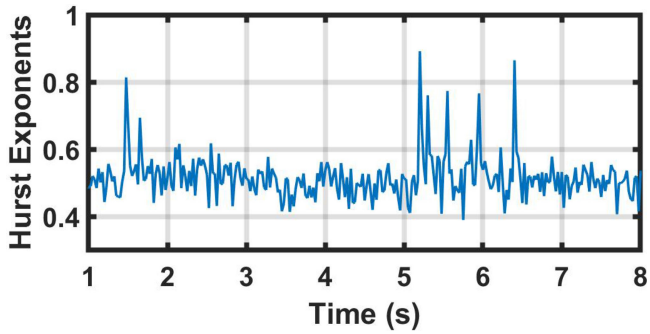

Fig. 14. Chaotic load profile immunity. A zoomed-in capture of Fig. 13.

(BPF range: 10–20 kHz). The corresponding Hurst exponent shows no false triggering and correctly detects the arc-ignition event. This was verified using 342 hardware test samples, which were collected previously and injected with switching noise.

C. DSP Implementation

After the algorithm was validated in MATLAB using the arcs database, the method was implemented using a DSP. First, the calculation load required by the proposed method is identified.

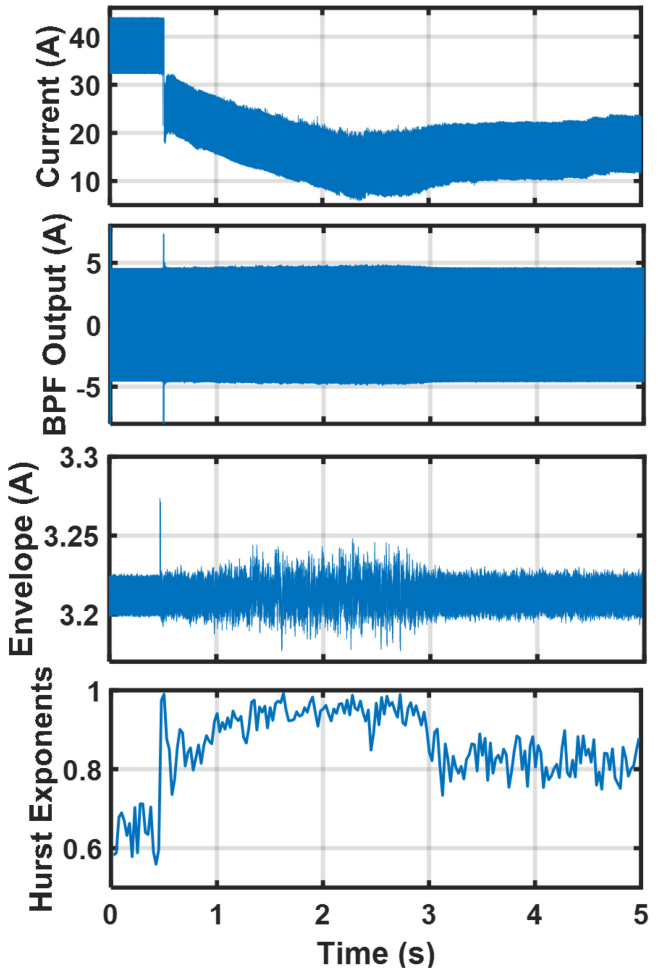

Fig. 15. Noisy dc arc occurring at 0.5 s with the corresponding Hurst exponents.

The processing power needed by the algorithm is mainly decided by the number of calculations performed for the sampled data, which is given by

$$\sum_{N=0}^{N=\frac{\ln n/2}{\ln 2}} \frac{12n}{2^{N+1}} \tag{6}$$

where n is the number of points per Hurst window. The number of points mainly depends on the Hurst exponent window size and the sampling speed. Higher sampling rate results in more accurate detection but higher calculation load. Table III shows a comparison of the calculation load for the proposed method with other methods [9]. The proposed method has a significantly lower number of calculations compared to the FFT and the other statistical method. This allows the proposed method to be implemented on various low-cost DSPs.

A prototype was built to implement the proposed method in hardware and validate the live detection of arc events. A sensor board with a BPF was designed and built, as shown in Fig. 16. The BPF is a second-order single-stage active filter with a slope of 40 dB per decade. The implemented BPF response is shown in Fig. 17. The envelop filter and the Hurst estimation were

TABLE III
CALCULATION LOAD COMPARISON WITH OTHER METHODS

Method	Calculation Load Per Window (FLOPS)	Sample Calculation, N=250 (FLOPS)
Fourier Transform	$5NLog_{(2)}N$	10 k
Statistical Entropy	24N	6 k
Proposed Method	$\sum_{N=0}^{N=\frac{\ln\frac{n}{2}}{\ln 2}} \frac{12n}{2^{N+1}}$	3 k

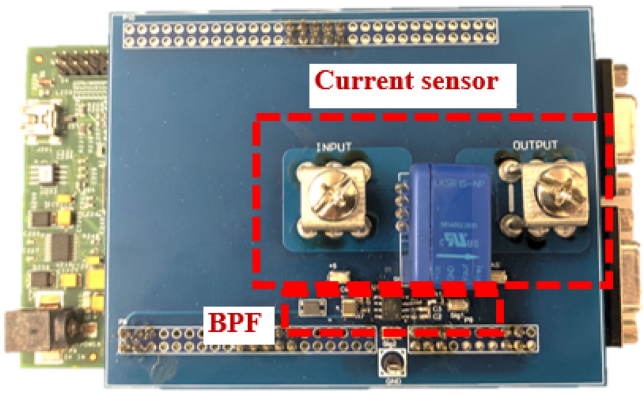

Fig. 16. Arc detector prototype.

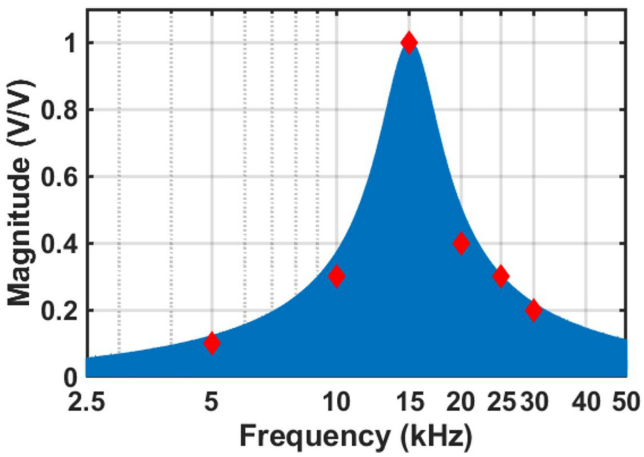

Fig. 17. Hardware BPF response. Cutoff frequency: 10–20 kHz. Blue: theoretical response. Red: experimental response.

implemented in software using a DSP. A total of 70 arc tests were performed at room temperature with the arc detector prototype. A 100% detection rate was achieved with a detection time of 50 ms using two Hurst windows (each window is 25 ms).

A sample test result is shown in Fig. 18. The arc can be observed occurring at $t = 1$ s. The DSP outputs a fault flag, which changes from low to high (0–3.3 V) when an arc is

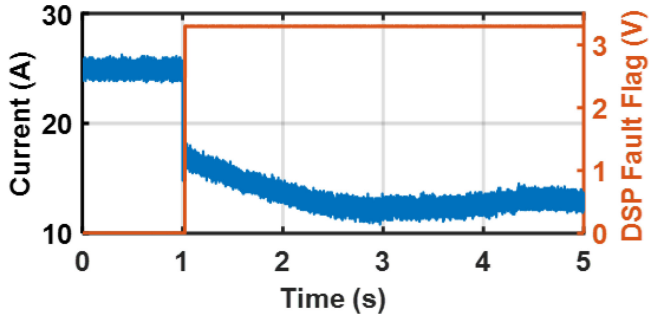

Fig. 18. Online detection of an arc occurring at $t = 1$ s using the prototype.

TABLE IV
ARC DETECTOR SPECIFICATIONS

Hardware	
Sensor Noise Level	≅ -40 dB
Band pass Filter Range	10 kHz < f_{PB} < 20 kHz
Sampling Rate	60 kHz
Software	
CPU Speed	150 MHz
CPU Core Count	1
RAM Usage	21.2 kB (66.25%)
Flash Usage	10.8 kB (4.22%)

TABLE V
DETECTION RATE

Sample Type	#of samples	Detection rate	Mistrigger rate
DC Arcs (Database)	342	100%	0%
Load Profiles	10	-	0%
Arcs With Live Detection	70	100%	0%
Overall	422	100%	0%

detected. The DSP changes the flag from low to high within 50 ms of the arc ignition. This validates the proposed method effectiveness for arc detection. Table IV shows the prototype specifications.

D. Detection Rate

To verify the reliability of the proposed method, a detection rate study was performed. First, a subset of 352 samples from the arcs database (room temperature tests) was used with MATLAB to test the detection rate of the method offline. Several load profiles were also tested to verify that no false triggering occurs. Then, the prototype was used to perform 70 tests for online detection. A summary of the tests is shown in Table V. The Hurst detection method was able to detect 100% of the arc events with zero miss-triggers for the arcs from the database (offline) and

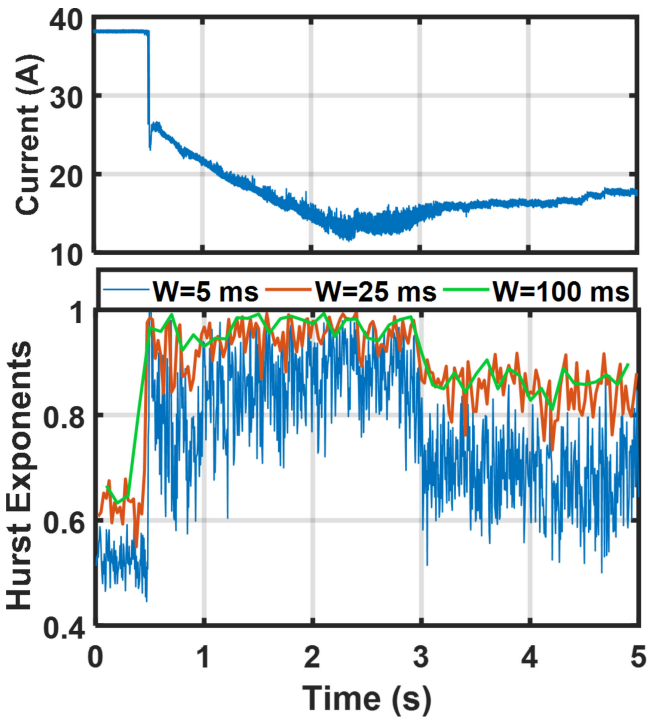

Fig. 19. Effect of the Hurst window size. Larger window results in more stable values but longer detection times.

the arc detector prototype (online detection) based on the test conditions from Table I.

E. Parameter Selection

To achieve a reliable arc detection, the detection parameters need to be properly selected. There are four main parameters affecting the method performance: BPF cutoff frequencies, envelope window, Hurst window, and number of Hurst windows for detection decision making.

The BPF and envelope filter mitigate the effects of load profiles and switching noises. Chaotic load-changing profiles are similar to dc arcs and can cause false positives. Switching noises acting like background noises can mask dc arc signatures and cause false negatives. The BPF (or high-pass filter) lower cutoff frequency is selected to remove low-frequency components in the load profiles, which is generally below 10 kHz in MHEVs. The higher cutoff frequency reduces influences of fast load-changing transients and suppresses high-frequency switching noises. It is selected as 20 kHz in the filter design.

The Hurst window is defined as the time duration, during which a Hurst exponent value is calculated. The Hurst window is selected based on a tradeoff between detection time sensitivity and detection accuracy. At time scales below 10 ms, the Hurst values become fluctuating due to current sensors limited bandwidth, sample rate, and signal-to-noise ratio. Increasing the Hurst window reduces the sensitivity of detection but improves the Hurst values stability against mis-triggers (false positives). This is shown in Fig. 19 with an arcing event at 0.5 s. It can be seen that the Hurst exponent results have a consistent increase (ΔH_{th} over 0.2) after the arc event when Hurst window is 25 ms (used in the arc detection). The number of Hurst windows used to determine a detection result is also a tradeoff between detection sensitivity and detection accuracy. A minimum of two windows is required to avoid mis-triggers.

The envelope filter mainly targets periodical switching noises. The window size of the envelope filter has to be larger than the period of the lower cutoff frequency of the BPF and smaller than the Hurst window, as written in (7). Because the BPF performance is not ideal, this value needs to be about ten times larger than the period of the cutoff frequency. After the envelope is applied, a small amount of white noise needs to be added. The white noise can be about 0.05% to 0.25% of the maximum system current. If the white noise is too high, the arc signature becomes harder to detect.

$$t_{\text{Hurst}} > t_{\text{ENV}} > 10/f_{\text{BPF,low}} \tag{7}$$

where t_{Hurst} and t_{ENV} are the Hurst and envelope window sizes, and $f_{\text{BPF,low}}$ is the lower cutoff frequency of the BPF.

VI. Conclusion

An improved detection method for high-impedance dc arcs using Hurst exponents with a two-stage filtering was proposed. The proposed detection method has strong system adaptability, high noise immunity, and low computational requirements. A dc arc generator setup was built based on a 48-V system, and more than 1000 tests were performed to generate dc arcs at different electrode diameters, loads, gap lengths, and environment temperatures. The hardware tests, in addition to chaotic load profiles and injected switching noise, were used to validate the method effectiveness and reliability for arc detection. An arc detector prototype was built, and the method was implemented on a DSP. It is shown that the method achieves a 50–100 ms detection time and 100% detection rate for the tests performed.

References

[1] S. Lee, J. Lee, W. Jung, Y. Park, and C. Won, "ZVT interleaved bi-directional low voltage dc-dc converter with switching frequency modulation for MHEV," in *Proc. 20th Int. Conf. Elect. Mach. Syst.*, Aug. 2017, pp. 1–6.

[2] R. Rong and R. Wang, "High efficiency 1.5kW 48V-12V dcdc converter with leadless MOSFET for mild hybrid electric vehicle," in *Proc. Int. Exhib. Conf. Power Electron., Intell. Motion, Renew. Energy Energy Manage.*, Jun. 2018, pp. 1–6.

[3] T. Kim and S. Baek, "Multiple bus motor drive based on a single inductor multi output converter in 48 V electrified vehicles," in *Proc. IEEE Int. Electr. Mach. Drives Conf.*, May 2017, pp. 1–6.

[4] U. Orji *et al.*, "Adaptive zonal protection for ring microgrids," *IEEE Trans. Smart Grid*, vol. 8, no. 4, pp. 1843–1851, Jul. 2017.

[5] T. J. Schoepf, M. Naidu, and S. Gopalakrishnan, "Mitigation and analysis of arc faults in automotive dc networks," *IEEE Trans. Compon Packag. Technol.*, vol. 28, no. 2, pp. 319–326, Jun. 2005.

[6] M. Naidu, T. J. Schoepf, and S. Gopalakrishnan, "Arc fault detection scheme for 42-V automotive dc networks using current shunt," *IEEE Trans. Power Electron.*, vol. 21, no. 3, pp. 633–639, May 2006.

[7] K. Lee, G. Seo, and B. Cho, "DC arc fault detection method for dc microgrid using branch monitoring," in *Proc. 9th Int. Conf. Power Electron./ECCE Asia*, Jun. 2015, pp. 2079–2084.

[8] Y. Gao, J. Zhang, Y. Lin, and Y. Sun, "An innovative photovoltaic dc arc fault detection method through multiple criteria algorithm based on a new arc initiation method," in *Proc. IEEE 40th Photovolt. Spec. Conf.*, Jun. 2014, pp. 3188–3192.

[9] G. Seo, J. Ha, B. Cho, and K. Lee, "Series arc fault detection method based on statistical analysis for dc microgrids," in *Proc. IEEE Appl. Power Electron. Conf. Expo.*, Mar. 2016, pp. 487–492.
[10] N. L. Georgijevic, M. V. Jankovic, S. Srdic, and Z. Radakovic, "The detection of series arc fault in photovoltaic systems based on the arc current entropy," *IEEE Trans. Power Electron.*, vol. 31, no. 8, pp. 5917–5930, Aug. 2016.
[11] Q. Sultana, P. Mishra, and S. Chary, "Novel control methodology for detecting series arc in dc circuits," in *Proc. IEEE 2nd Int. Conf. DC Microgrids*, Jun. 2017, pp. 12–17.
[12] S. Chae, J. Park, and S. Oh, "Series dc arc fault detection algorithm for dc microgrids using relative magnitude comparison," *IEEE J. Emerg. Sel. Topics Power Electron.*, vol. 4, no. 4, pp. 1270–1278, Dec. 2016.
[13] A. Shekhar, L. Mackay, L. Ramrez-Elizondo, and P. Bauer, "Experimental design of a series arc load side detection algorithm for dc microgrid protection," in *Proc. Int. Symp. Power Electron., Elect. Drives, Autom. Motion*, Jun. 2016, pp. 343–347.
[14] L. Yuan, J. Shengchang, W. Jin, Y. Xiu, and Z. Yeye, "Study on characteristics and detection of dc arc fault in power electronics system," in *Proc. IEEE Int. Conf. Condition Monit. Diagnosis*, Sep. 2012, pp. 1043–1046.
[15] X. Yao, L. Herrera, S. Ji, K. Zou, and J. Wang, "Characteristic study and time-domain discrete- wavelet-transform based hybrid detection of series dc arc faults," *IEEE Trans. Power Electron.*, vol. 29, no. 6, pp. 3103–3115, Jun. 2014.
[16] Z. Wang and R. S. Balog, "Arc fault and flash signal analysis in dc distribution systems using wavelet transformation," *IEEE Trans. Smart Grid*, vol. 6, no. 4, pp. 1955–1963, Jul. 2015.
[17] X. Yao, L. Herrera, Y. Huang, and J. Wang, "The detection of dc arc fault: Experimental study and fault recognition," in *Proc. 27th Annu. IEEE Appl. Power Electron. Conf. Expo.*, Feb. 2012, pp. 1720–1727.
[18] X. Yao, L. Herrera, and J. Wang, "Impact evaluation of series dc arc faults in dc microgrids," in *Proc. IEEE Appl. Power Electron. Conf. Expo.*, Mar. 2015, pp. 2953–2958.
[19] G. Seo, K. A. Kim, K. Lee, K. Lee, and B. Cho, "A new dc arc fault detection method using dc system component modeling and analysis in low frequency range," in *Proc. IEEE Appl. Power Electron. Conf. Expo.*, Mar. 2015, pp. 2438–2444.
[20] R. D. Telford, S. Galloway, B. Stephen, and I. Elders, "Diagnosis of series dc arc faults—A machine learning approach," *IEEE Trans. Ind. Inform.*, vol. 13, no. 4, pp. 1598–1609, Aug. 2017.
[21] M. Chen *et al.*, "Detection method of low voltage series dc arc based on the pattern matching algorithm," in *Proc. 20th Int. Conf. Elect. Mach. Syst.*, Aug. 2017, pp. 1–4.
[22] Y. Abdullah, B. Hu, W. Zhou, Y. Wang, J. Wang, and A. Emrani, "Hurst exponent-based adaptive detection of dc arc faults," in *Proc. IEEE Energy Convers. Cong. Expo.*, Oct. 2017, pp. 2645–2650.
[23] Y. Abdullah, B. Hu, Z. Wei, J. Wang, and A. Emrani, "Adaptive detection of dc arc faults based on hurst exponents and current envelope," in *Proc. IEEE Appl. Power Electron. Conf. Expo.*, Mar. 2018, pp. 3392–3397.
[24] X. Yao, L. Herrera, L. Yue, and H. Cai, "Experimental study of series dc arc in distribution systems," in *Proc. IEEE Energy Convers. Congr. Expo.*, Sep. 2018, pp. 3713–3718.
[25] H. Namazi *et al.*, "A signal processing based analysis and prediction of seizure onset in patients with epilepsy," *Oncotarget*, vol. 7, pp. 342–350, 2016.
[26] Y. Alperovich, M. Alperovich, and A. Spiro, "Trends modeling and its impact on hurst exponent at stock market fractal analysis," in *Proc. 10th Int. Conf. Manage. Large-Scale Syst. Develop.*, Oct. 2017, pp. 1–4.
[27] J. Bassingthwaighte and G. Raymond, "Evaluation of the dispersional analysis method for fractal time series," *Ann. Biomed. Eng.*, vol. 23, pp. 491–505, 1995.

Yousef Abdullah (Student Member, IEEE) received the B.S degree in electrical engineering from Kuwait University, Kuwait City, Kuwait, in 2013, and the M.S. degree in 2016 from the Ohio State University, Columbus, OH, USA, where he is currently working toward the Ph.D. degree mainly focusing on power electronics applications of GaN devices and electromagnetic interference.

His research interests include motor drives, power inverters for photovoltaic systems, and microgrids.

Jamie Shaffer received the bachelor's degree in computer engineering from Miami University, Oxford, OH, USA, in 2018. He is currently working toward the master's degree in electrical engineering with The Ohio State University, Columbus, OH, developing a high-speed optimization system for aircraft dc microgrids.

His interests include dc–dc converter design, energy storage management, and system control.

Boxue Hu (Member, IEEE) received the B.S. degree from the Harbin Institute of Technology, Harbin, China, in 2011, the M.S. degree from the Institute of Electrical Engineering, Chinese Academy of Sciences, Beijing, China, in 2014, and the Ph.D. degree from The Ohio State University, Columbus, OH, USA, in 2019, all in electrical engineering.

He is currently a Research Associate with the Center for High Performance Power Electronics, The Ohio State University. His research interests include applications of wide-bandgap semiconductor devices, partial discharge detection in medium-voltage systems, and dc arc fault detection and protection.

Bailey Hall received the B.S. degree in electrical and computer engineering from Miami University, Oxford, OH, USA, in 2017. He is currently working toward the Ph.D. degree, under the advisory of Dr. J. Wang, with the Ohio State University, Columbus, OH, USA.

His current interests include series dc arc prevention and the electrification of modern aircrafts.

Jin Wang (Senior Member, IEEE) received the B.S. degree from Xi'an Jiaotong University, Xi'an, China, in 1998, the M.S. degree from Wuhan University, Wuhan, China, in 2001, and the Ph.D. degree from Michigan State University, East Lansing, MI, USA, in 2005, all in electrical engineering.

From September 2005 to August 2007, he was a Core Power Electronics Engineer with the Ford Motor Company. In 2007, he joined as an Assistant Professor with the Ohio State University, Columbus, OH, USA, where he was promoted to an Associate Professor in 2013, and a Full Professor in 2017. He has more than 190 peer-reviewed journal and conference publications and nine patents. His research interests include wide-bandgap power devices and their applications, high-voltage and high-power converter/inverters, integration of renewable energy sources, and electrification of transportation.

Dr. Wang received the IEEE Power Electronics Society Richard M. Bass Young Engineer Award in 2011, the National Science Foundation's CAREER Award in 2011, and the Nagamori Award in 2020. At the Ohio State University, he received the Ralph L. Boyer Award for Excellence in Undergraduate Teaching Innovation in 2012, the Lumley Research Award in 2013, and the Harrison Faculty Award for Excellence in Engineering Education in 2017. He served as the General Chair and the Steering Committee Chair for the IEEE Future Energy Challenge in 2016 and 2017, respectively. He was an Associate Editor for the IEEE TRANSACTIONS ON INDUSTRY APPLICATIONS from 2008 to 2014. He has served in many leading conference organization committees. He initiated and served as the General Chair for the 1st IEEE Workshop on Wide Bandgap Power Devices and Applications in 2013. He currently serves as the Tutorial Co-Chair for the 2020 IEEE Applied Power Electronics Conference, and an Associate Editor for the IEEE TRANSACTIONS ON POWER ELECTRONICS and the IEEE JOURNAL OF EMERGING AND SELECTED TOPICS IN POWER ELECTRONICS.

Amin Emrani (Member, IEEE) was born in Isfahan, Iran, in 1985. He received the B.S. and M.S. degrees in electrical engineering from the Isfahan University of Technology, Isfahan, in 2007 and 2010, respectively, and the Ph.D. degree from Binghamton University, Binghamton, NY, USA, in 2014.

He has several years of experience in various areas from machine learning, data science, and image processing to power electronics and solid-state fabrication. He has work experience with Fortune 100, start-up companies, and academia, including R&D positions with Ford Motor Company, Palo Alto, CA, USA, and Cornell University, Ithaca, NY. Throughout his professional career, he has been leading, conducting, and contributing to several interdisciplinary research projects, which led to more than 26 technical publications and patents, which have been cited more than 290 times.

Babak Arfaei received the Ph.D. degree in materials science and engineering from Binghamton University, Binghamton, NY, USA, in 2010.

He is currently a Materials Scientist with Ford Motor Company, Palo Alto, CA, USA, and also a Research Assistant Professor with the Physics Department, Binghamton University. Prior to Ford, he worked with Universal Co., where he conducted research in the area of reliability of electronic packages. His research interests include, additive manufacturing, 2-D materials, microstructure and texture analysis of metals, nucleation and growth in metallic systems, and thermomechanical behavior of lead-free solder alloys.

Dr. Arfaei is a member of the Technical Committee of Surface Mount Technology Association (SMTA) and the Electronic Packaging and Interconnection Materials Committee of The Minerals, Metals & Materials Society (TMS). He serves as a Technical Advisor for the *Journal of the Minerals, Metals, and Materials* (JOM) as well as a Reviewer for multiple international publications.